REVIEW ARTICLE

Magnetic Fields to Enhance Tuned Liquid Damper Performance for Vibration Control: A Review

Andrea Vázquez-Greciano[1,2] · Antonio Aznar López[1] · Nicola Buratti[2] · Jesús María Ortiz Herrera[1]

Abstract

Tuned Liquid Dampers (TLDs) are dissipative devices whose distinguished features like low cost in installation and maintenance or their multidirectional and multifrequency application to new and already existing structures make them an attractive damping option. Their working principle is similar to that of a Tuned Mass Damper but in this case the relative movement comes from a fluid that provides with mass, damping and stiffness. Moreover, TLDs can mitigate both horizontal and vertical vibrations. All these make TLDs worth deeply studying. TLD utilization in civil vibration control arose in the 1980s. From early years, different improvements have been implemented to achieve a better performance. Some of these modifications include passive variations in the geometry or the fluid. The use of smart materials applied on TLDs has also been of great interest since the 1990s and comprehends different configurations in which magnetic fields are used to passively or semi-actively improve the TLD performance. A lack of review is detected in this field. For this reason, a state-of-the-art review is presented in this paper. Its aim is to help researchers find a thorough, up-to-date classification of the different possibilities, configurations, numerical evaluation, materials used and also found limitations and future development in the application of magnetic fields on TLDs.

Keywords Tuned Liquid Damper · Smart material · Magnetic field · Structural vibration control

1 Introduction

The reduction of vibrations in structures is a central topic in civil engineering. Vibration may arise either during exceptional events, i.e. earthquakes, explosions etc., or in service conditions, i.e. pedestrian loads on footbridges, vehicles loads on bridges, etc. Depending on the source of vibration different mitigation techniques are to be used, because they have different objectives.

For instance, the main objective in case of earthquakes is to ensure life safety during these rare events that induce a limited number of large-amplitude vibration cycles, therefore solutions based on hysteretic damping and on the exploitation of ductility can be implemented [1, 2], even if they produce structural damage. Vibrations associated to operational conditions require different solutions since they are associated to a very high number of cycles and must produce no damage.

The well-known failure of the Tacoma Narrows Bridge (Washington) in 1940 [3] or the closure right after the inauguration of the Millennium Bridge (London) in the year 2000 [4] are examples that highlight the importance of vibration control, since vibration complications can even appear during construction and if detected afterwards may result in significant changes in the structure and in high costs, not only in materials but also due to loss in usable area.

Passive structural control systems present an alternative to conventional methods by dissipating the energy produced by a dynamic loading or isolating the main

Antonio Aznar López, Nicola Buratti and Jesús María Ortiz Herrera have contributed equally to this work.

✉ Andrea Vázquez-Greciano
  andrea.vazquez.greciano@upm.es

  Antonio Aznar López
  antonio.aznar@upm.es

  Nicola Buratti
  nicola.buratti@unibo.it

  Jesús María Ortiz Herrera
  jesusmaria.ortiz@upm.es

[1] Department of Building Structures and Physics, Universidad Politécnica de Madrid, Pº Juan XXIII, 11, 28040 Madrid, Spain

[2] Department of Civil, Chemical, Environmental and Materials Engineering, Alma Mater Studiorum Università di Bologna, Via Zamboni, 33, 40126 Bologna, Italy

structure, and therefore modifying the amount of energy that finds its way into the system, resulting in a reduction of the internal forces the structure is subjected to [2]. Among the dissipative devices fall Tuned Mass Dampers (TMDs) and Tuned Liquid Dampers (TLDs) [5]. These are secondary systems that add one degree of freedom when attached to a primary structure. Consequently, the natural frequencies of the structure are modified, and its behavior can be controlled within the elastic range in periodic actions for an everyday response mitigation.

TMDs rely on the out-of-phase movement of a mass with respect to the main structure, hence the energy exchange between the main structure and the device. The TLDs working principle is similar to that of TMDs. In this case, the relative movement is provided by a fluid in a container which provides a secondary mass, damping and stiffness on its own with no need for external supplemental devices, which make TLDs an attractive dissipative mechanism alternative.

TLDs were first employed in marine vessels in the beginning of the 20th century [6] and their applications were expanded to space satellites in 1960s [7, 8] and to offshore platforms in the 1970s [9]. It was during 1980s that they were used efficiently on civil structures such as towers and bridges [10, 11]. Bauer [11] introduced a vibration absorber that consists of a rigid container filled to the top with two immiscible liquids whose densities differ and thus shift the natural frequency of the device in order to allow tuning to that of the system. Its mathematical and mechanical model was developed, showing that the movement occurs in the interfacial surface, while the relative velocity of layers next to the walls equals zero. Therefore, the model could be represented by sloshing masses of the n-th mode connected to the side walls by springs at a certain height above the bottom of the container and non-moving masses located at the top and bottom. These are commonly referred to as Tuned Sloshing Dampers (TSDs) since their behavior is characterized by the sloshing of a fluid inside a tank, generally in rectangular, circular, or annular shape, although other geometries that fit the available space have also been considered [12].

Another variation of TLDs are Tuned Liquid Column Dampers (TLCDs), that were developed in the 1990s [13, 14]. These damping mechanisms have also been investigated for wind turbines [15] and offshore platforms [16, 17]. Traditionally, these consist of a U-shaped tube filled with water that mitigates the structure vibration through the gravitational restoring force that acts on the displaced fluid. Damping is obtained through viscous interaction between the fluid and the container and head loss due to flow through orifices on the device.

Successful implementations of TLDs in different configurations all over the world include among others: bridges, like the Toda Park Bridge [18, 19] or the Ikuchi Bridge (Japan) [20]; towers, such as the Nagasaki Airport Tower, Yokohama Marine Tower, Shin-Yokohama Prince Hotel, Tokyo International Airport Tower in Japan [21], the Sky Tower in Auckland (New Zealand) [22], Brighton i360 Viewing Tower in the United Kingdom [23], One King West Tower in Toronto [24] and One Wall Center in Vancouver (Canada) [25], One Rincon Hill Tower in San Francisco [26] and Comcast Center Tower in Philadelphia (United States) [27]; and also smaller scale implementations on facades like Notre Dame de Pentecôte in Paris (France) [28] or even sculptures, such as "My World and Your World" in London (United Kingdom) [29].

TLDs present several advantages over other types of damping devices, such as: low cost in installation and maintenance since they have no moving parts, applicability in both permanent and temporal installations in either new or already existing buildings, no-limitation to unidirectional vibration suppression, easiness to tune by varying the geometry of the container or the depth of the liquid and effectiveness for small-amplitude applications.

They do however present some disadvantages that need to be taken into consideration. In the case of shallow TSDs, only a fraction of the total fluid mass takes part in reducing the structure's motion. This fact, together with water's low density means the space required to be installed is larger when compared to a TMD. Moreover, water presents a low inherent damping that is not enough to reach the desired optimum value and nonlinear sloshing behavior makes it difficult to predict specially if wave breaking occurs.

Different approaches to overcome these difficulties and to enhance TLDs behavior have been developed from early years. Passive modifications remain aligned with the properties that make TLDs remarkable, and include variations in the fluid used, in the container shape or in their arrangement. The use of smart materials applied on TLDs has also been of great interest since the 1990s and comprehends different configurations in which magnetic fields are used to passively or semi-actively improve the TLD performance. A lack of review is detected in this field of study. For this reason, a state-of-the-art review is presented in this paper to help researchers find an up-to-date classification of the different possibilities, configurations, materials used and also found limitations in order to facilitate further research in this field.

As guidance to fully understand the impact of each approach improvement, the basic TMD and TLD formulations are first studied due to their similarities. Next, a thorough classification of the different passive enhancement mechanisms of TLDs is presented, followed by a detailed review of the existing literature and working-type classification for the utilization of smart fluids subjected to magnetic fields on TLDs. Lastly, the key aspects of TLDs with magnetic fields, their limitations and future development are discussed.

2 TMD Working Principle

As guidance to better understand TLDs behavior and enhancement possibilities, TMD formulation is presented due to their similarities. TMDs are well known passive vibration control devices largely used to protect civil structures against external dynamic events. In their simplest form, they consist of a mass-spring-dashpot system attached to a structure as depicted in Fig. 1.

Mass vibration absorbers were first proposed by Frahm in the early 20th century by means of a supplemental mass attached to a single degree of freedom structure through a spring [30]. When the main mass is subjected to periodic vibrations with a frequency equal or close to the natural frequency of said system, increased amplitude vibrations occur due to resonance. These vibrations can be suppressed upon the application of a secondary mass that is tuned to the natural frequency of the main structure due to an out-of-phase movement of the secondary mass with respect to the primary mass. TMDs take damping into account, which allows to delimitate the amplitude response to finite values [31].

Frahm mass vibration absorber helps understand the effect of the inclusion of a secondary mass. The equations of motion of both the main and secondary systems (as depicted in Fig. 2) are defined in Eqs. (1) and (2) respectively when an external sinusoidal dynamic force *F(t)* is applied to the structure.
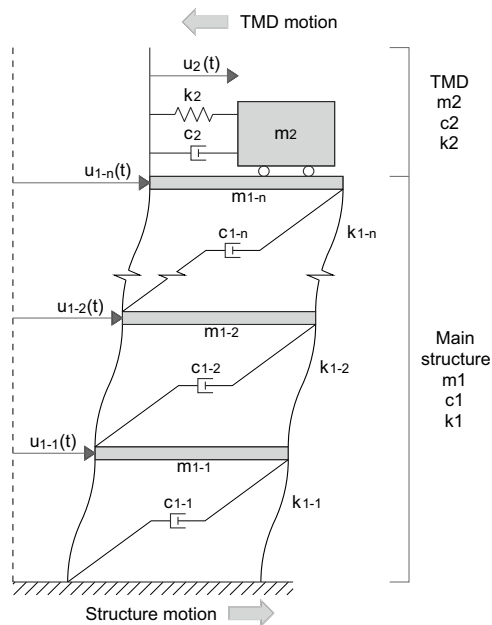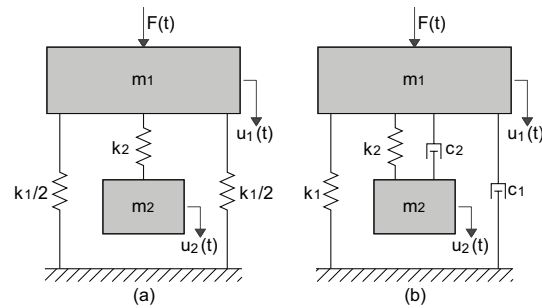

Fig. 2 Mass dissipative devices, **a** Frahm vibration absorber model, **b** Tuned Mass Damper model

$$m_1\ddot{u}_1 + k_1 u_1 + k_2(u_1 - u_2) = F_0 sin(\omega t)$$
$$= F(t) \tag{1}$$

$$m_2\ddot{u}_2 + k_2(u_2 - u_1) = 0 \tag{2}$$

Solving these equations, the responses of the main and secondary systems are (Eqs. 3 and 4):

$$u_1(t) = A_1 sin(\omega t) \tag{3}$$

$$u_2(t) = A_2 sin(\omega t) \tag{4}$$

Obtaining the derivatives of Eqs. (3) and (4) and considering that the natural frequency can be defined as $\omega_n^2 = k_n/m_n$, for an external vibration frequency equal to the natural frequencies of the main and secondary systems, $\omega = \omega_1 = \omega_2$, we obtain that $A_1 = 0$ and $A_2 = -F_0/k_2$, meaning that the main system amplitude is nullified since the secondary spring is applying a force $-F_0$ that cancels $F(t)$ on the main system, as seen in Fig. 2a. The inclusion of a secondary mass on a structure adds one degree of freedom to the system, and therefore generates two new natural frequencies centered on the original one.

Another interesting parameter that arises from these calculations is the mass ratio, defined as the ratio of the secondary mass to the primary mass, $\mu = m_2/m_1$. From Fig. 3 it can be seen that larger mass ratios enlarge the frequency band in which TMDs are effective. Typical values are considered to be around μ = 1-5% [32, 33], although higher values can also be considered [34] setting the optimum maximum on around μ =10% [35].

Proceeding similarly when damping is accounted for, the equations of motion can be expressed as in Eqs. (5) and (6) and it can be seen in Fig. 3b that the amplitude of vibration of the main system is diminished around resonance and it is reduced to finite values on the new frequencies. The typical damping ratio, $\xi = c/(2m\omega)$, of a TMD system is approximately ξ =3.5% [36, 37].

Fig. 1 TMD attached to a structure

$$m_1\ddot{u}_1 + c_1\dot{u}_1 + k_1u_1 + c_2(\dot{u}_1 - \dot{u}_2)$$
$$+ k_2(u_1 - u_2) = F_0sin(\omega t) = F(t) \tag{5}$$

$$m_2\ddot{u}_2 + c_2(\dot{u}_2 - \dot{u}_1) + k_2(u_2 - u_1) = 0 \tag{6}$$

3 TLD Working Principle

TLDs working principle is similar to that of TMDs. In this case, the relative movement is provided by a fluid in a container which provides with a secondary mass, damping and stiffness on its own with no need for external supplemental devices. Its working principle can be seen in Fig. 4.

In the following subsections a summary of TSD and TLCD formulation is presented to facilitate understanding

the modelling of TLDs and the impact of their enhancement possibilities.

3.1 TSD Formulation

The schematic of a TSD can be seen in Fig. 5 representing rectangular and cylindrical containers respectively. Fig. 6 depicts the two main design models developed by Housner and Yu et al. and a more recent combination of both of them [38–41].

Further theoretical developments of mathematical models to describe the liquid motion of TSDs, that were experimentally validated for free oscillations and harmonic driving forces, were carried out in the 1980-90s [42–46]. Nonlinear shallow water wave theory was shown to be effective for small amplitudes and for continuous free surface, this means, when no weave breaking occurs. Small amplitudes are those below
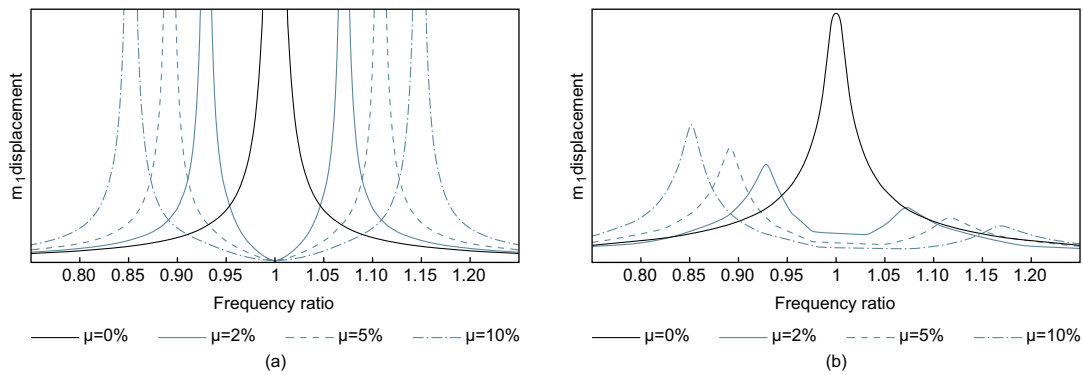

Fig. 3 m_1 displacement response for various mass ratios, **a** Frahm vibration absorber model, **b** Tuned Mass Damper model
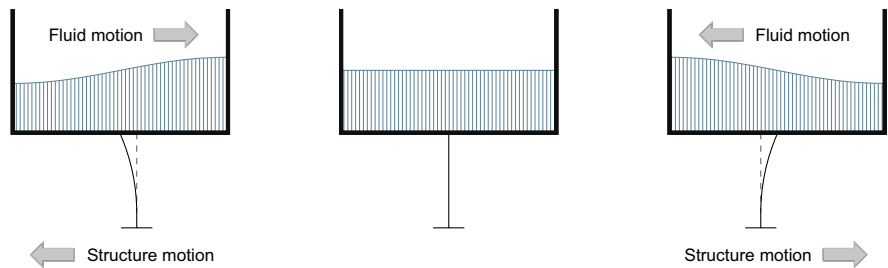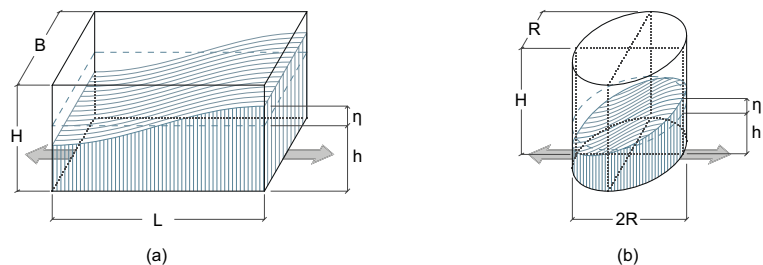

Fig. 4 Working principle of TLDs

Fig. 5 TSD schematics, **a** Rectangular TSD dimensions, **b** Cylindrical TSD dimensions
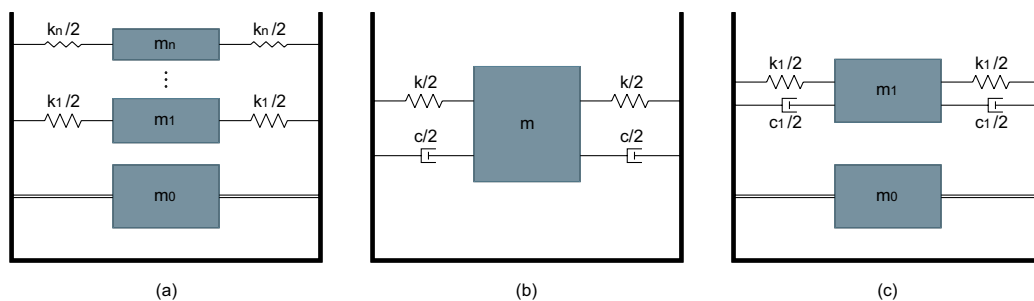
Fig. 6 TSD models, **a** Housner model, **b** Yu et al. model, **c** Combined model

1% of the TSD length L. Amplitudes over 2% of the TSD length are considered large [47].

Shallow water is referred to as relations between the length of the tank in the direction of motion L ($L=2R$ in the case of circular base) and the fluid depth h, $h/L < 0.15$. In shallow containers the response wave height is similar to the depth of the fluid and therefore nonlinearities need to be taken into consideration [48]. On the contrary, in deep water containers ($h/L > 0.15$) the response wave height is small compared to the fluid depth, and thus nonlinear terms can be ignored.

Although more easily nonlinear, shallow TSDs reach smaller frequencies, are activated even for small amplitudes and most of the fluid mass participates in the sloshing. On deep containers the frequency range is augmented, and their behavior can remain linear for a larger range of amplitudes [49], but there is a larger fraction of the mass that does not participate in the sloshing, adding unusable damping weight to the main structure.

TSD behavior can be explained by the hydrodynamic fluid pressures developed under horizontal accelerations. The total mass can be divided into an impulsive (non-effective) mass whose pressures are related to the forces of inertia on the walls, and a convective (effective) mass, that occurs due to sloshing [39]. The impulsive mass (m_0) is considered to be rigidly attached to the container and moves alongside with it. The convective masses ($m_{1,n}$) can be represented by masses for different modes connected to the container through a spring, as depicted in Fig. 6. The spring has a stiffness K that can be calculated for each mode from Eq. (7) [50] and depends on the mode mass and frequency. For most cases, the sum of the impulsive mass and the first convective mass represents over 95% of the total mass (m_{tot}).

$$k_i = m_i(2\pi f_{i,TSD}) \tag{7}$$

The formulation of the equivalent masses was developed in the 1950s [39] and is adopted in various design codes [50–52]. The impulsive mass m_0 and the first convective mass m_1 are defined in Eqs. (8) and (9) for rectangular and cylindrical containers.

$$m_0 = \frac{h}{\kappa_0} tanh\left(\frac{\kappa_0}{h}\right) m_{tot} \tag{8}$$

$$m_1 = \frac{\kappa_{11}}{h} tanh\left(\frac{h}{\kappa_{12}}\right) m_{tot} \tag{9}$$

where κ takes the values κ_{0R} and κ_{0C} for the impulsive mass and the values κ_{11R}, κ_{12R}, κ_{11C} and κ_{12C} for the first convective mass of rectangular and cylindrical containers respectively (see Table 1).

One of the first publications regarding the damping contribution of surface waves in containers [53] suggests that viscous damping occurs not only near the rigid walls of the container, both bottom and side walls, but is also generated from the free surface layer contamination and capillary hysteresis on the contact between the previous parts.

Early studies state that shallower liquid in TSDs results in higher damping [43, 54]. This is further explained by Habenberger [55], who defines the proportion in which the viscosity of the fluid and the containers walls and base take part in the overall damping ratio. Damping in shallow tanks arises from bottom friction while damping in deep tanks occurs mainly due to the fluid motion on the side walls.

The damping coefficient of fluid sloshing based on linear wave theory for a rectangular tank is defined in Eq. (10) [43, 56, 57]. It is affected by the wave surface elevation η, the fluid depth h and tank width B, the convective mass m_1, the fluid kinematic viscosity v, its angular frequency ω_{TSD} and a surface contamination factor S that takes the value $S=1$ for a fully contaminated surface [40, 43].

Table 1 Values for k

Impulsive mass m_0		Convective mass m_1			
k_{0R}	k_{0C}	k_{11R}	k_{12R}	k_{11C}	k_{12C}
1.7L/2	1.7 R	0.26 L	L/3.2	0.33 R	R/1.8

$$c_{TSD} = \frac{m_1}{\sqrt{2}(\eta + h)}\sqrt{\nu\omega_{TSD}}(1 + \frac{2h}{B} + S) \tag{10}$$

It can be deduced from Eq. (10) that the damping ratio ξ_{TSD} decreases for higher values of fluid depth h, meaning that shallow containers should give higher damping ratios. Wave breaking is another cause of damping [54] that is not accounted for in Eq. (10).

It has been proven experimentally that both the stiffness and damping are not linear but increase with the amplitude of the excitation and a model was proposed by Yu et al. [38]. This is due to the fact that the effective damping ratio is proportional to the horizontal velocity of the particles [44].

TMDs damping ratio typically takes values of ξ=3.5% [36, 37]. TSDs can be modelled as equivalent TMD systems, and their optimum damping ratio is considered to be around 5-6% [47, 54, 58, 59] depending on the mass ratio μ, which represents the effective mass of the TLD to generalized mass of the structure in the mode of vibration considered. Taking this into consideration, it must be noted that the damping ratio for water and other fluids is considered to be $\xi = 0.5\%$ [60], which is rather low. Therefore, damping is a key factor that needs to be accounted for.

The value for the optimum damping ratio of vibration absorbers is defined as a function of the mass ratio μ and can be deduced from Eqs. (11), (12) and (13) for optimum displacement, velocity, and acceleration control respectively [35, 61]. It is worth noting that the maximum damping possible does not necessarily correspond to its optimum value. For instance, over increasing the damping on TSDs by means of an exceedingly viscous fluid would eventually make the sloshing mass become clamped together with the main structure mass, thus eliminating any relative movement between the secondary mass (TSD convective mass) and the main mass (structure).

$$\xi_{opt,x} = \sqrt{\frac{3\mu}{8(1 + \mu)^3}} \tag{11}$$

$$\xi_{opt,\dot{x}} = \sqrt{\frac{3\mu(1 + \mu + \frac{5\mu^2}{24})}{8(1 + \mu)\left(1 + \frac{\mu}{2}\right)^2}} \tag{12}$$

$$\xi_{opt,\ddot{x}} = \sqrt{\frac{3\mu}{8(1 + \frac{\mu}{2})}} \tag{13}$$

Being the frequency tuning ratio ($\Omega = f_{TSD}/f_{structure}$) a key parameter in the proper functioning of TLDs, the frequency of sloshing of TLDs must be defined. The optimal Ω is in the range 0.95−1.04 [48] and comes from Eqs. (14), (15) and (16) for optimum displacement, velocity, and acceleration control respectively [35, 61].

$$\Omega_{opt,x} = \frac{1}{1 + \mu} \tag{14}$$

$$\Omega_{opt,\dot{x}} = \frac{\sqrt{1 + \frac{\mu}{2}}}{1 + \mu} \tag{15}$$

$$\Omega_{opt,\ddot{x}} = \frac{1}{\sqrt{1 + \mu}} \tag{16}$$

According to linear wave theory [43, 54], the frequency of sloshing in rectangular and cylindrical containers are defined in Eqs. (17) and (18) respectively. It depends only on the geometrical characteristics of the tanks, their length L or radius R, the height of fluid h and the gravitational acceleration g and variables that define the modes.

$$f_{R-TSD} = \frac{\omega_{R-TSD}}{2\pi} = \frac{1}{2\pi}\sqrt{\frac{\alpha_n g}{L}tanh\left(\frac{\alpha_n h}{L}\right)} \tag{17}$$

$$f_{C-TSD} = \frac{\omega_{C-TSD}}{2\pi} = \frac{1}{2\pi}\sqrt{\frac{\lambda_n g}{R}tanh\left(\frac{\lambda_n h}{R}\right)} \tag{18}$$

The parameters α_n and λ_n are set for the different modes. The variable α_n used for rectangular containers is defined as $\alpha_n = \pi(2n - 1); \alpha_1 = \pi, \alpha_2 = 3\pi, \alpha_3 = 5\pi, \alpha_4 = 7\pi \ldots$ and the variable λ_n used for cylindrical containers is obtained from the zeros of the of the first derivative of the Bessel function of the first kind of order 1; $\lambda_1 = 1.8412, \lambda_2 = 5.3314, \lambda_3 = 8.5363, \lambda_4 = 11.7060 \ldots$ [50, 62]. It must be noted that although higher frequencies can be reached in higher modes, the liquid mass that participates in the higher modes of sloshing in a TSD is low as compared to that of the fundamental mode [63].

3.2 TLCD Formulation

The schematic of a TLCD is depicted in Fig. 7. TLCDs exploit the movement of the liquid as it oscillates between the two columns. For its modelling it is considered that sloshing does not occur on the columns and that the fluid is incompressible [64].

The first interesting difference from TDSs is that on TLCDs the total mass participates in the dissipative device, thus all the mass can be considered effective (Eq. (19)).

$$m_{TLCD} = \rho A L \tag{19}$$

Considering a unit change in the water level, the restoring force produced by gravity can be computed as (Eq. (20)):
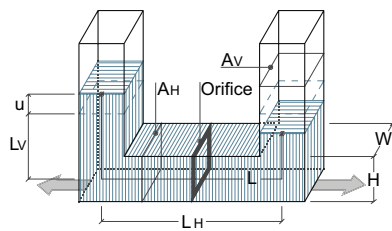
Fig. 7 Schematic view of a TLCD

$$k_i = m(2\pi f_{TLCD})^2 = 2\rho Ag \qquad (20)$$

which can be interpreted as the stiffness of the system. Therefore, the natural frequency of the system is (Eq. (21)) [65, 66]:

$$f_{U-TLCD} = \frac{1}{2\pi}\sqrt{\frac{2g}{L}} \qquad (21)$$

where g indicates the gravity constant and L is the total fluid length as seen in Fig. 7.

TLCDs are generally U-shaped, although other geometries, such as V-shape have also been studied [67].

The damping coefficient c can be defined as (Eq. (22)) [68–70]:

$$c = \sqrt{\frac{2}{\pi}}\frac{m\delta}{L}\sigma_{\dot{x}} \qquad (22)$$

It depends on the fluid mass m, the length L, the overall head loss coefficient δ, and the standard deviation σ of the fluid velocity $\dot{x}$ on the flow channel, this is, the measurement of the dispersion of the fluid velocity values along the tube.

The head loss coefficient δ represents the amount of energy that is lost on a fluid flowing through a pipe due to its velocity, the dimensions of the pipe and a friction factor that depends on the roughness of the tube and the Reynolds number [71].

Experimental investigations have been carried out to obtain the head loss coefficient and to evaluate the influence of the opening ratio of the orifice (measured as the ratio between the orifice gap and the horizontal section height) on the damping [68] and it is concluded that smaller opening ratios, especially for values below 0.5, increase the damping coefficient and that small orifice openings better control the fluid motion and thus prevent splashing outside of the container. It has been seen that the damping also increases with the amplitude of the movement of the water columns [68]. The amplitude-dependency of the damping ratio can be explained considering that at smaller amplitudes, viscous interaction between the fluid and the tank is the main mechanism of energy dissipation. On the contrary, flow separation and turbulence induced at higher liquid velocities and

Reynolds number occur under larger amplitudes of vibration [72].

As for optimization, similar criterion to TSDs is followed [69].

4 TLD Passive Improvements

Passive modifications remain aligned with the properties that make TLDs remarkable, and include variations in the fluid used, in the container shape or in their arrangement. A classification of the different approaches for TSDs and TLCDs if presented in the following subsections.

4.1 TSD Enhancement

The necessity to increase the damping arose early in the development of TLDs since water presents a damping ratio coefficient ξ=0.5% [60], which is rather low compared to optimum values of around 5% [58]. Different approaches to overcome this drawback have been studied, and the first passive modifications include:

- Variations in the fluid
- Variations in the container
- Considering wave breaking

4.1.1 Variations in the Fluid

TSDs usually contain water, which can also be used as a reservoir in case of undesired events such as fire. However, it has been shown that the use of other fluids con improve performance of TSDs against vibration suppression.

Different fluid viscosities, varying from water to fluids presenting 30 times the viscosity of water, were first experimentally discussed in the late 1980s by Sun et al. [73]. Experiments showed the previous nonlinear shallow water wave theory could be effectively applied to high-viscosity fluids and that the more viscous the fluid, the smaller the wave height of the sloshing and thus evidencing viscosity can be used to prevent wave breaking [74]. It is also noted that viscosity increases the damping ratio and, if excessive, may result in poorer performance of the TSD [44, 48, 73]. High density and viscosity heavy mud has also been considered [58]. Its viscosity is velocity-dependent and has been successfully implemented on a reinforced concrete bridge pier to suppress wind vibration during construction.

The contribution on damping of density together with viscosity has been recently studied [75]. Different commercially available fluids (e.g. water, acetone, chloroform, propanol, mercury···) were considered and an Adaptative Harmony Search algorithm was used to optimize the fundamental period, damping, length and height of the container

for all the fluids so that the minimum displacement of the main structure was obtained for each case. It was concluded that the fluid choice is strongly related to the mass of the main structure: for single degree of freedom structures the best behavior was achieved with the smallest kinematic viscosities followed by smallest density values; for a 40-storey structure, the smallest kinematic viscosity and highest density fluids reduced the movement the most.

4.1.2 Variations in the Container

Varying the container base shape or height and including obstacles in the liquid flow such as screens, baffles, wedges or obstacles, as depicted in Fig. 8, are means to increase the damping and therefore the energy dissipation. One of the first publications in this field considers roughness of the bottom of the container and suggested that the elements studied did now imply an increment in additional damping but did seem to vary the tuning frequency [45] as a result of a fluid depth modification.

Rough tank base in the form of symmetrical wedges at the bottom of the container has also been considered for various wedge surface configurations [76] and it was concluded that when stepped or holed, better damping performance was achieved compared to plain wedges. In recent years 3D printed blocks have been used to modify the tank base shape [77, 78]. The frequency and damping ratio variations with respect to the water depth ratio (*h/L*) for different bottom container shapes have also been examined [77]. It becomes evident that the water depth ratio is a crucial parameter: higher frequencies can be reached for higher values of *h/L* while this results in smaller damping ratios. It is worth

mentioning sloped bottoms were seen to provide a damping ratio twice as big as flat-bottomed containers.

Sloshing against the roof of the container is a way to dissipate energy. It has been reported how the limitation in height of the tank affects the effectiveness of TSDs [45, 79, 80]. Very limited heights may reduce the effectiveness of TSDs, and it is generally advised to account for a freeboard height of 1−1.5 times the fluid depth to avoid restraining the fluid motion [45] since additional damping derived from roof impact results in a poorer TSD performance [79]. In this field, floating roofs have also been reported [81, 82] not as means to increase the damping but to prevent water from breaking and to ensure more predictable TSDs with linear behavior and amplitude-independent parameters.

The passive practice of including obstacles was first studied in the 1990 s adding lattice screens in the middle section of the tank [83]. Both theory and experiments demonstrate the inclusion of the screens results in more linear behavior and internal damping augmentation of the TSD. Tait et al. [59] add a series of horizontal slats and define mass, damping and frequency as amplitude dependent parameters. Various static elements such as poles and screens have been successfully implemented on residential tower buildings [84, 85].

4.1.3 Considering Wave Breaking

Although highly nonlinear, weave breaking enhances the damping. In order to account for this behavior, two experimental coefficients were introduced in the equation of motion by Sun et al. [56] modifying the damping and frequency (see Eqs. (23) and (24)). The frequency modifying coefficient is almost constant while the damping modifying
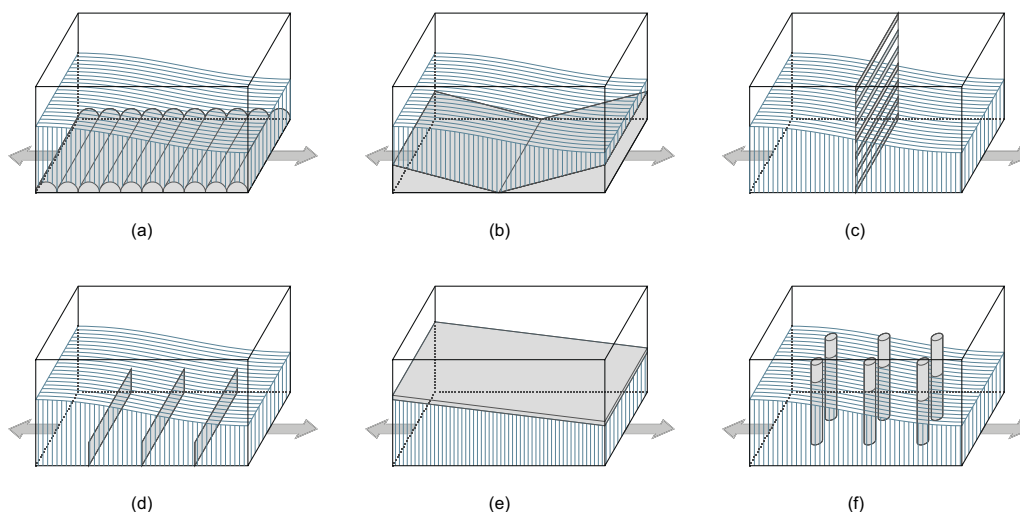
Fig. 8 Variations on the TSD container, **a** TSD with rough bottom, **b** TSD with wedges, **c** TSD with screens, **d** TSD with baffles, **e** TLCD with floating roof, **f** TLCD with poles

coefficient depends on the frequency of sloshing *f*, the base amplitude *A*, the fluid height *h* and the density ρ and dynamic viscosity μ of the fluid. It is worth mentioning that larger base amplitudes result in not only greater energy dissipation but also occurs over a broader frequency band [46]. Further studies to predict free surface nonlinear behavior were carried out by Frandsen [86].

$$C_{frequency} \approx 1.05 \tag{23}$$

$$C_{damping} = 0.57 \sqrt{\frac{2\pi f A \rho 2h^2}{L\mu}} \tag{24}$$

Recently, a novel way of inducing wave breaking and mobilizing convective mass has been reported [87]. It consists of the inclusion of a submerged pendulum in deep containers and allows for a hybrid TMD-TSD system if tuned to different frequencies.

4.2 TLCD Enhancement

TLCDs properties can be further enhanced in different ways. Some approaches seek to increase their damping and other seek a better adaptability to space restrictions or aim to reach higher frequencies or to suppress vertical motion. Depending on the passive alterations imposed, variations can be classified as follows:

- Variations in the fluid
- Variations in the container shape
- Variations in the container arrangement
- Variations in the orifice
- Considering sealing

4.2.1 Variations in the Fluid

Different fluids can provide with diverse upgrades. The use of anti-freezing liquids is of interest to ensure the fluid movement. A water-glycol fluid, similar in density to water but with a dynamic viscosity 18 times higher, performance has been studied [88] and it was seen that ever though the

water-glycol fluid has higher viscous damping, the response reduction was similar to that of water.

The use of dense fluids to enhance the damping effect is stated as preferable [89]. How different fluid densities suppress the structure motion has been considered and experimentally validated [90]. In the case of study, more dense fluids showed better behavior since, for the same volume, the mass ratio increases.

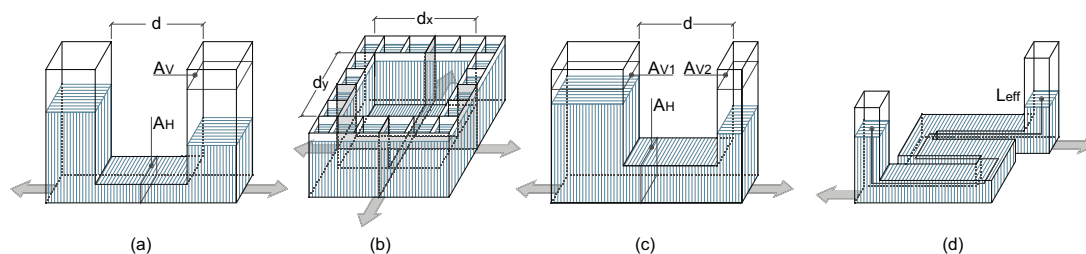### 4.2.2 Variations in the Container Shape

In the search of better adaptability, Liquid Column Vibration Absorbers (LCVAs), as depicted in Fig. 9a and 9b, were developed in the 1990s [67, 72, 91]. The tuning frequency of LCVAs is defined by an effective length that considers the differences in geometry of the horizontal and vertical sections (see Eqs. (25) and (26)). This makes it possible to create smaller TLCDs that are suitable for long period structures.

$$f_{LCVA} = \frac{1}{2\pi} \sqrt{\frac{2g}{L_{eff}}} \tag{25}$$

$$L_{eff} = \frac{A_V}{A_H} d + 2L_V \tag{26}$$

Uni- [72, 92] and bi-directional [91] LCVAs have been studied and validated experimentally under free vibration tests that were used to define how the geometrical parameters affect the frequency and damping ratio. It was seen that bigger values for the area ratio (A_V/A_H) yielded bigger damping ratios which are also amplitude dependent. The horizontal section length d is not a cause for variations of the damping ratio. The effect of viscosity is also studied utilizing fluids whose viscosity is up to 40 times greater than that of water. As expected, these did not affect the natural frequency. The damping ratio was seen to slightly increase for higher values of viscosity.

Further modifications of LCVAs have been studied [93] considering different cross-sectional areas of each column

Fig. 9 Variations on the TLCD container shape, **a** unidirectional LCVA, **b** bidirectional LCVA, **c** asymmetric LCVA, **d** S-shaped TLCD
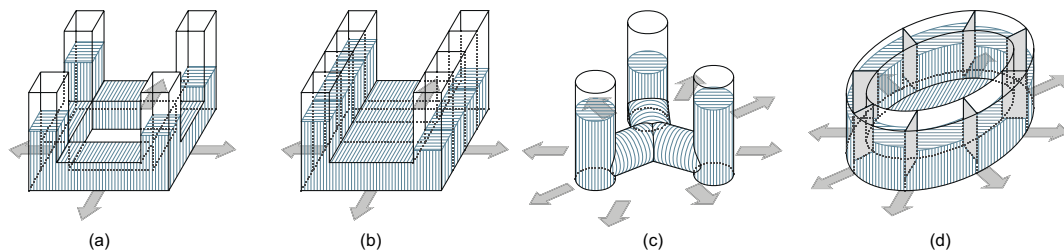
Fig. 10 Variations on the TLCD container arrangement, **a** bidirectional TLCD, **b** bidirectional TLD+TMD, **c** inter-connected multidirectional TLCD, **d** toroidal TLCD

creating an asymmetry parameter that modifies the frequency, as seen in Fig. 9c.

Another variation to increase the effective length is obtained through an S-shaped horizontal section [16] as depicted in Fig. 9d, which allows to increase the effective length without taking up long linear space.

The inner shape of TLCDs can also be modified including roughness. The inclusion of embossments has been studied as means to increase the damping coefficient [94].

### 4.2.3 Variations in the Container Arrangement

Traditional TLCDs are aimed at suppressing unidirectional movements but can be rearranged to conform multidirectional dissipative devices, as seen in Fig. (10). In this regard, bidirectional TLCDs have been developed and studied experimentally [95, 96]. Their combination allows for smaller amount of fluid needed when compared to individual TLCDs. The model proposed by Min et al. [96] (Fig. 10b) behaves as a TLCD in one direction and as a TMD in the perpendicular direction because the fluid mass is accounted for in the direction in which its sloshing is restricted.

Multi-direction TLCDs have also been proposed in the shape of inter-connecting vertical columns [97] or toroidal containers that have been validated experimentally [98–100] (Fig. s 10c and 10d). It must be noted that while multi-direction control has the advantage of suppressing movements in any arbitrary direction, their reduction is not as effective as their traditional TLCD counterpart for the aimed unidirectional movement.

Regarding frequency tuning, multiple TLCDs (MTLCDs) have been proposed as means to control the maximum displacements [101] and to prevent malfunctioning from mistuning [102]. MTLCDs are tuned to various frequencies around the natural frequency of the structure so that the sensitivity of the system to the tuning ratio is reduced. When put together, as seen in Fig. 11, multi-column TLCDs (TLMCDs) can also be tuned to various frequencies and take up less space than MTLCDs [103–105].
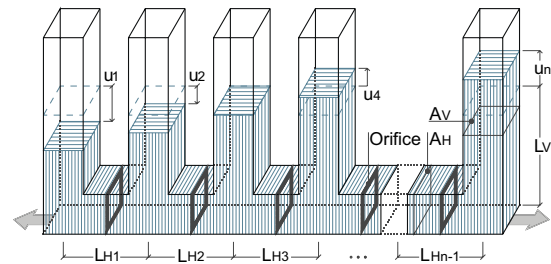
Fig. 11 Tuned Liquid Multi Column Damper
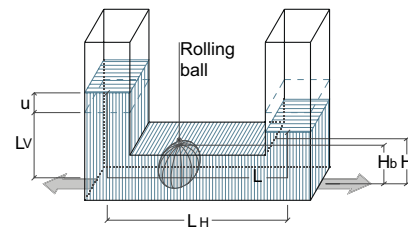
Fig. 12 TLCD with ball acting as a moving orifice

4.2.4 Variations in the Orifice

A rolling ball in the horizontal section of the TLCD acting as a moving orifice has also been considered [106, 107] and is shown in Fig. 12. In this case energy dissipation is enhanced since it is caused by resistance to flow, friction between the fluid and the ball and kinetic energy of the rolling ball. Increasing the ball diameter increases in turn the damping and a value of 0.8 with respect to the horizontal section heigh is found as optimum [106]. Different ball densities have been taken into consideration and it was seen that denser materials improved the vibration reduction [90]. Furthermore, the ball motion can be controlled by a spring. This proposal enhances TLCD performance and prevents the ball from hitting the lateral walls [108] and has been developed numerically and validated experimentally [109].

4.2.5 Considering Sealing

Apart from horizontal vibrations, vertical vibrations can occur and cause discomfort, like the ones produced by pedestrians walking on a bridge. TLCDs have been studied to control vertical vibrations of this type [89, 110–112]. A gas spring model is developed for this purpose and applied to TLCDs, obtaining the so-called Tuned Liquid Column Gas dampers (TLCGDs) in which a section is sealed, and a gas pressure is imposed, as shown in Fig. 13.

The natural frequency of a TLCGD, defined in Eq. (27), depends on the geometrical characteristics of the tank and on a modified stiffness provided by the pressurized gas, also known as air spring stiffness, which highly influences the restoring forces [113, 114]. The variable h_0 denotes an equivalent atmospheric air column for equilibrium and n represents the polytropic index. It is worth mentioning that TLCGDs can reach higher frequencies (up to 5 Hz) [115].

$$
\begin{aligned}
f_{TLCGD} &= \frac{1}{2\pi}\sqrt{\frac{2g}{L_{eff}}sin\beta + \frac{gn(2H_0 + h_0)}{L_{eff}H_a}} \\
&= \sqrt{\frac{2g}{L_{eff}}sin\beta + \frac{p_0 n}{L_{eff}H_a\rho}}
\end{aligned}
\tag{27}
$$

Air spring chambers can also be used on to combine TLCGDs that can be used for multi-mode tuning to several frequencies [115] and can improve TLMCDs efficiency by applying different air pressure (50-100 bar) on different columns [116].

5 Magnetic Fields Applied on TLDs

Some of the passive modifications previously presented can also be achieved though magnetic fields. As stated before, since water has low viscosity and relatively low density, TLDs need to be larger to achieve the same level of performance of TMDs and if unmodified do not reach the optimal damping value. One approach to enhance the performance of TLDs is to use smart materials that overcome these drawbacks, thus creating a light damper with the addition of a magnetic field. Smart materials are those that respond in a controllable and reversible way to external stimuli by altering some of their properties. Among this category fall field responsive fluids that can be further classified into magnetorheological (MR), electrorheological (ER), and ferro-fluids [117–120].

Smart fluids have been used in the automotive, aerospace, and optical polishing industries and anti-shock devices [117, 119, 121, 122] and their operating principle is similar to hydraulic dampers in which damping comes from the pressure that is required to force a fluid through an orifice [123].

Regarding building and civil engineering, smart fluids are mainly used in hydraulic cylinders for seismic response mitigation [124] and have been experimentally studied [125]. This kind of application has been recently reviewed by Lenggana et al. [126]. Their first full-scale applications took place in the early 2000 s on the Nihon-Kagaku-Mirai-kan Building in Tokyo and the Dongting Lake cable-stayed Bridge in China [127, 128]. Vertical motion suppression MR dampers of buildings under seismic activity have been reported by Cesmeci et al. [129].

With respect to TLDs, including both TSDs and TLCDs, different configurations including magnetic fields have been studied theoretically and experimentally since the 1990s to enhance their performance against undesired vibrations. A lack of review is detected in this field of study. For this reason, a state-of-the-art review is presented in this paper to help researchers find an up-to-date classification of the different possibilities, configurations, materials used and also found limitations in order to facilitate further research in this field.

5.1 Field Responsive Fluids

Field responsive fluids are briefly presented in this section with the aim of introducing their main features and differences.

5.1.1 Magnetorheological (MR) Fluids

MR fluids were first reported in the late 1940s by Rabinow [117, 119–121, 130]. They are composed of micron-sized

Fig. 13 Tuned Liquid Column Gas Damper, **a** inner chamber, **b** end chamber
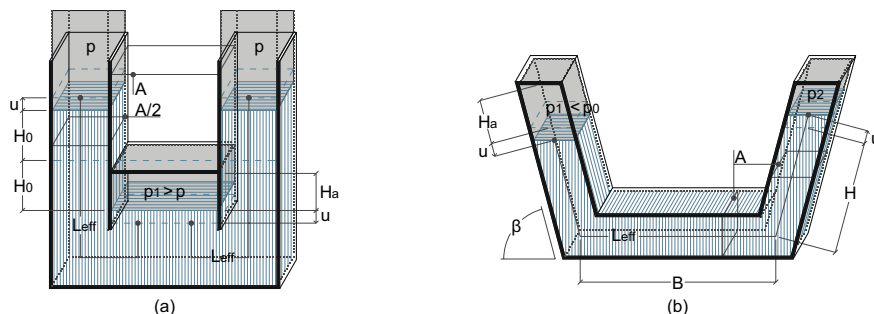
magnetizable particles (1–10 μm) and additives dispersed in a base fluid.

Diverse metal and alloy compositions, like MnZn or NiZn ferrites or FeCo alloys, have been described as the magnetically active phase. Nevertheless, high purity iron powder is the most frequently used magnetic material [117, 119]. The carrier fluid is generally aqueous or silicon, mineral or synthetic oil based, and ought to be non-reactive against the particles as well as having a low temperature-independent viscosity. Additives are required to regulate suspension and include stabilizers and surfactants.

Some aspects of MR fluid rheology can be modified upon the application of an external magnetic field. During the off-state they flow freely, and the particles become polarized and rearrange into chain-like structures in the same direction as the applied magnetic field in the on-state [117, 119, 120, 131–133] as shown in Fig. 14. This setting results in an increment of the viscosity (up to 105-106 times) in milliseconds that can be reversed when the magnetic field is no longer present. MR fluids develop yield stresses with values around 100 kPa [118, 134].

5.1.2 Electrorheological (ER) Fluids

ER fluids were developed in the 1940s by Winslow [119, 121, 135] and are composed of dielectric micron-sized particles (1-100 μm), such as titanate, silica, or zeolites, suspended on non-conductive fluids like silicone oil. Under the influence of an electric field, the particles become polarized and align into chain-like structure, rapidly and reversibly increase the fluid viscosity [118, 119, 135]. ER fluids develop yield stresses of about 5-10 kPa [118, 134].

5.1.3 Ferrofluids

Rosensweig [136] defines magnetic ferrofluids as stable synthetized colloids of ferrite particles in suspension in a non-reactive continuous medium. The nano-sized (2-10 nm) magnetic particles are covered with a dispersant layer that prevents agglomeration and settling and, unlike MR and ER fluids, ferrofluids do not develop yield stress and remain flowing under the influence of a magnetic field [118, 119,

Fig. 14 MR fluid behavior, **a** off-state, **b** on-state

136, 137]. Their variations in viscosity due to the applied magnetic field are reviewed in Doganay et al. and Genc and Derin [138, 139].

5.1.4 Other Types of Smart Fluids

Commercial smart fluids tend to be costly when compared to other industrially available fluids of various viscosities. For this reason, some authors have attempted at developing said fluids form commercially available materials [140]. Another type of low-cost smart fluids are photo-rheological fluids whose viscosity decreases in presence of UV light [141].

5.2 Magnetic Field TLD Working Types

In the field of TLDs, the study of magnetic fluid sloshing arose during the development of space technology [142].

Wave dynamics and the effects of uniform and non-uniform magnetic fields on ferrofluids are studied theoretical and experimentally by Zelazo and Melcher [143] who experimentally quantify the shift in resonance frequency of a ferrofluid sloshing in a rectangular container moving horizontally when a magnetic field is imposed normally and tangentially. They suggest a proportional relation between the natural sloshing frequency of the fluid and the magnetic field applied.

Sudo et al. [142] study the response of the water-based ferrocolloids when vibrated horizontally in a rectangular container under the application of a magnetic field tangential to the horizontal free surface of the fluid (both normal and parallel to the direction of vibration). It was seen that the amplitude of surface waves decreased with increasing intensity of magnetic field due to the formation or particle chains oriented along the direction of the applied field and that the resonant frequency was intensity dependent.

Sawada et al. [144] study the behavior of a magnetic fluid in a sinusoidally oscillating rectangular tank when a non-uniform vertically oriented magnetic field is applied. The frequency of sloshing is determined by a modified gravity value that arises from the application of the magnetic field force. An increase of the magnetic field results in a reduction of the velocity profile of the fluid [145].

The different working types in which magnetic fields applied on TSDs and TLCDs to control structure vibration subjected to dynamic loads are identified. The following classification is proposed (fig. 15):

- TSD horizontal magnetic field: parallel, perpendicular, multidirectional
- TSD vertical magnetic field: bottom and alternating top and bottom
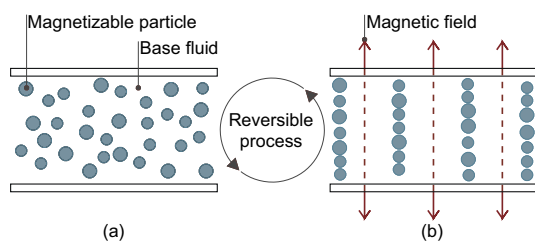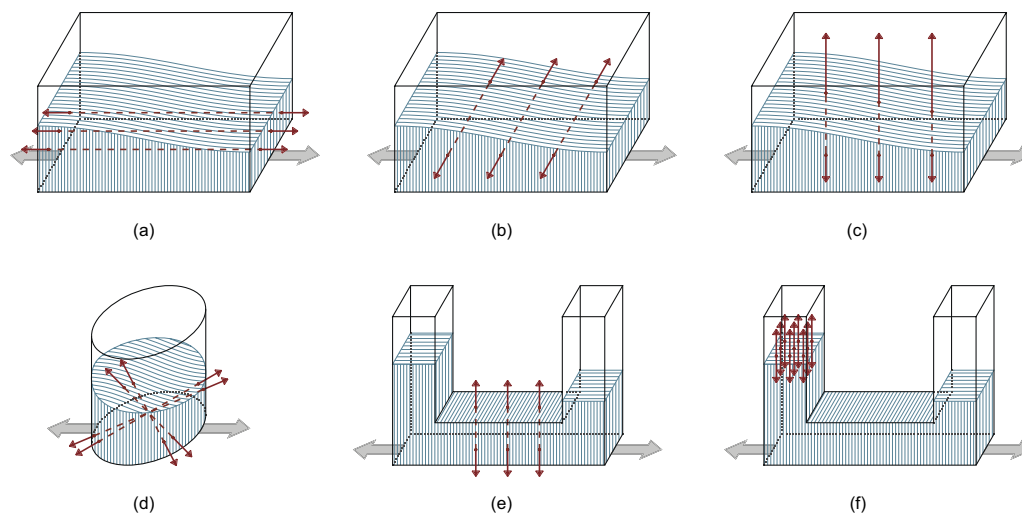- TLCD horizontal section
- TLCD vertical section

Fig. 15 Classification of TLDs including magnetic fields, **a** TSD with horizontal magnetic field parallel to motion, **b** TSD with horizontal magnetic field perpendicular to motion, **c** TSD with vertical magnetic field, **d** TSD with multidirectional magnetic field, **e** TLCD with magnetic field on horizontal section, **f** TLCD with magnetic field on vertical section
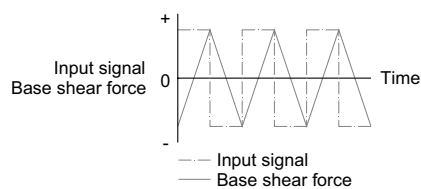
Fig. 16 Time history of input signal and base shear force with a 90° phase lag

5.2.1 TSD Horizontal Magnetic Field

To the best of found knowledge, the first study regarding the application of magnetic fields on TSDs to mitigate vibrations of a building model was published by Abé et al. [146]. Horizontal magnetic field implementations vary from passive to active devices and can be classified depending on the orientation of the magnetic field with respect to the motion of the structure. This section first presents parallel to motion applications, followed by multi-directional and perpendicular implementations.

Magnetic fields applied parallel to the direction of motion seek an improvement of the vibration suppression of passive TSDs by means of a dynamic magnetic field. This type of application allows to enhance or suppress sloshing as required by means of an alternating magnetic field.

For electromagnets located at each side of a rectangular tank aligned with the direction of the displacement, there is a phase delay between the alternating applied magnetic field and the base shear force exerted by the TSD [146, 147], as depicted in Fig. 16.

The frequency of sloshing is calculated according to linear wave theory, as presented in section 3, and is not affected by the magnetic field.

Rule-based controlled active dynamic application of magnetic fields on TSDs attached to a model scale building is studied by Abé et al. [146, 148]. In this case, an 8 mT magnetic field is applied horizontally along the direction of motion. For a unity tuning ratio between the frequency of excitation and the frequency of sloshing, a 90-degree phase lag between the input signal and the base shear force response is observed. This property is similar to that of a single degree of freedom linear oscillator subjected to harmonic excitation, implying that base shear force can be controlled by similar control laws [148] defined in Eq. (28):

$$u = -u_{max}sgn[x(1 - c\alpha)] \tag{28}$$

where x is the structure displacement, c is a control constant and α depends on the structure and fluid displacement and velocity and the natural frequencies of the structure and TSD. Larger values of α suggest larger response of the TSD in comparison with the structure and vice versa. This comprehension allows to reduce the TSD response if excessive and to enhance it if insufficient.

Horie et al. [147] propose a model in which the sloshing mass of the TSD is divided into effective (or convective) and non-effective (or impulsive) masses, whose quantities vary depending on the intensity of the magnetic field applied. The non-effective mass is enlarged under the application of the magnetic field. This arises from the formation of chain-like structures that restrict the movement, transforming convective mass into impulsive mass that rigidly moves along with

the structure, as shown in Fig. 17. This application makes it possible to adjust the mass ratio and thus providing with the capability to widen and narrow the effective frequency band.

Also, a reduction in the convective mass results in an enlargement of the damping ratio as seen in Eq. (29):

$$\xi = \frac{c}{2m_{eff}\omega_{TSD}} \tag{29}$$

Ohira et al. [149] apply multidirectional horizontal magnetic fields obtained from two pairs of electromagnets that are rotated with respect to the direction of motion of the structure to a cylindrical container filled with water-based magnetic fluid. They develop an analytical model to compute the behavior of the TSD using a TMD analogy and also divide the fluid mass into an effective and non-effective mass. The numerical model is validated experimentally. It is demonstrated that different phase delays of $\pm 90°$ of the applied magnetic field with respect to the velocity of the main structure respectively imply decreases on the first and second resonance peaks. An actively switching magnetic field condition near resonance improves the structural response since both peaks decrease in magnitude.

The distinct characteristic of solidifying when subjected to an electric or magnetic field of ER and MR fluids respectively leads to another particular application on TSDs. By means of a horizontal, perpendicular to motion magnetic field, Sakamoto et al. [150] use an ER fluid and control the effective tank length L_{eff} with electrodes as shown in Fig. 18.

This enables modifications of the frequency of sloshing (see Eq. (30)) thus efficiently controlling the response of the experimental steel frame for more than one resonant frequency.

$$f_{H-MF,perp} = \frac{1}{2\pi}\sqrt{\frac{\pi g}{L_{eff}}tanh\left(\frac{\pi h}{L_{eff}}\right)} \tag{30}$$

5.2.2 TSD Vertical Magnetic Field

Magnetic fields can also be installed vertically for a horizontally vibrating tank. The various applications of vertical
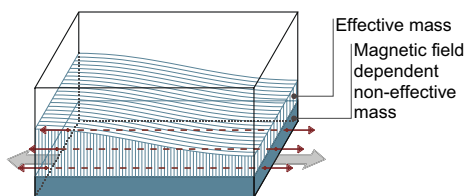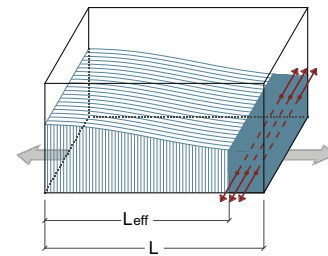

Fig. 18 Variation of the effective length of a TSD with horizontal, perpendicular to motion magnetic field

magnetic fields for a horizontally vibrating tank can be further categorized based on the location of said field. This section first presents vertical magnetic fields applied at the bottom of the container followed by and alternating top-bottom implementation.

Several authors [62, 144, 151, 152] examine the effect of a vertical magnetic field located at the bottom of laterally sloshing rectangular and cylindrical containers filled with various magnetic fluids. The equations that characterize the waves are similar to those that define the fluid motion of TSDs with the inclusion of an effective gravitational acceleration $g*$ that is modified by the vertical magnetic field [62, 144, 151].

Therefore, the first natural horizontal frequency of a magnetic fluid sloshing in a rectangular tank resulting from the application of a vertically oriented magnetic field is defined in Eq. (31),

$$\begin{aligned} f_{V-MF,n} &= \frac{\omega_{V-MF,n}}{2\pi} \\ &= \frac{1}{2\pi}\sqrt{\frac{\alpha_n g*}{L}tanh\left(\frac{\alpha_n h}{L}\right)} \end{aligned} \tag{31}$$

taking $\alpha_n = \alpha_1 = \pi$ and can be modified for a cylindrical container substituting L for R and α_n for λ_n and taking $\lambda_n = \lambda_1 = 1.8412$ [50, 62]. Vertical sloshing also occurs, and its natural frequency is obtained by substituting λ_n for λ_{Vn} and taking $\lambda_{V1} = 3.1387$ [62] (see Fig. 19).

The effective gravity $g*$ is defined in Eq. (32) as a function of the gravitational acceleration g, the vacuum magnetic permeability μ_0, an experimental constant β, the fluid
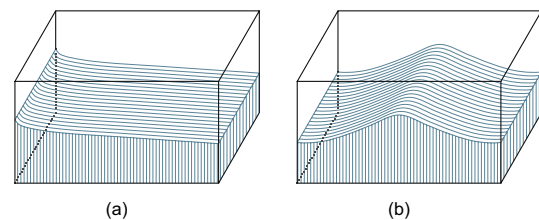

Fig. 17 Effective and non-effective mass of a TSD under a horizontal, parallel to motion magnetic field

Fig. 19 Types of sloshing **a** Horizontal sloshing, **b** Vertical sloshing

density ρ and magnetic susceptibility χ, the height h and the magnetic field intensity at the lowest part of the tank H_0.

$$g^* = g + \frac{\mu_0 \beta \chi H_0^2 e^{-2\beta h}}{\rho} \tag{32}$$

From these equations and proven by experiments developed by several authors [144, 151] it can be seen that the natural frequency can increase in the presence of a vertical magnetic field. This implies that higher frequencies, normally unreachable for this kind of device [153], could be obtained with the help of stronger magnetic fields and lower fluid densities.

The inclusion of a vertical magnetic field also helps control the fluid surface displacement η, defined by Eq. (33). X_0 and ω are the excitation amplitude and angular frequency. The maximum displacement of the free surface is seen to decrease upon the application of a vertical magnetic field [144].
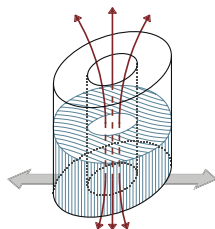
$$\eta = \frac{X_0 \omega^2 tanh\left(\frac{\pi h}{L}\right)}{\omega_{V-MF}^2 - \omega^2} \tag{33}$$

In the case of coaxial cylindrical containers studied by Ohno et al. [152] and represented in Fig. 20, it becomes clear that when hollow, the maximum magnetic field is not applied to the liquid (but the gap) and so the change rate of the sloshing frequency is smaller compared to a cylindrical container. This behavior can be improved if a Fe core is inserted in the hollow section to help spread the magnetic field.

Another source to dissipate maximum energy arises from wave breaking which helps keeping the magnetic particles dispersed. However, the fluid behavior becomes difficult to predict. In this field of study Frandsen [154] experimentally considers base harmonic excitations on steady vertically oriented magnetic fields for square containers and considers Lenz's law to explain the braking or drag force resulting from the conductor fluid moving perpendicularly to a steady magnetic field and thus creating a magnetic field opposing the applied one.

Horie et al. [147] experimentally studied the effect of vertically placed electromagnets at the top and bottom of a container used independently and it was seen that the individual

use of the upper and lower electromagnets would be beneficial for frequency ratios below and above 1 respectively.
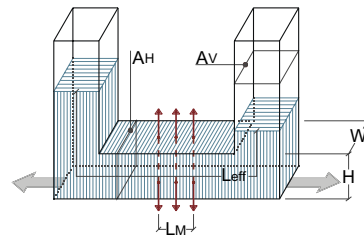
5.2.3 TLCDs Horizontal Section

Higher vibration mitigation is sought on TLCDs by implementing an external magnetic field. When located on the horizontal section of the TLCD, the damping ratio can be controlled. A mathematical model was first developed by Wang et al. [155] as well as several prototypes for a semi-active MR TLCD. The magnetic field is located at the bottom horizontal part of the TLCD filled with MR fluid, acting vertically as shown in Fig. 21.

TLCDs damping relies on the liquid flowing through an orifice with head loss characteristics and from viscous interaction between the liquid in motion with a certain velocity and the container walls. Substituting the orifice by the concentrated magnetic field, the motion of the fluid flowing through the horizontal section affected can be described in turn by the parallel-plate theory, namely valve working mode (see Fig. 22).

The magnetic field is applied orthogonally to the flow and modifies the velocity profile [156]. The pressure drop ΔP is a sum of a viscous rheological and a MR (magnetic field-dependent) component (Eq. (34)).

$$\Delta P = \Delta P_{VR} + \Delta P_{MR}$$
$$= \frac{12\mu Q L_M}{H^3 W} + \frac{\tau_{MR} L_M \gamma}{H} \tag{34}$$

This implies that the pressure drop depends on the dynamic viscosity μ of the fluid, the flow rate Q, the length of the

Fig. 21 Main dimensions of TLCD with magnetic field acting vertically on the horizontal section

Fig. 20 Coaxial cylindrical container with vertical magnetic field applied at the bottom of the tank
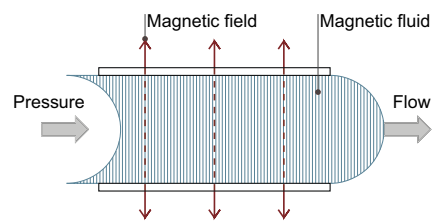
Fig. 22 Valve mode

magnetic field L_M and the gap height H and width W of the flow channel, the variable yield stress τ_{MR} as a response to the magnetic field, and an empirical coefficient γ which is a function of the flow velocity and takes values ranging from 2 to 3 [155, 157, 158]. It is to be noted that MR fluids should be used in this type of application since their damping enhancement relies on the developed yield stress.

Cheng et al. [159] take into consideration different viscosities of the MR fluid with diverse iron-particles concentrations. Larger content fractions of magnetic particles are more significantly influenced by the magnetic field. It is worth mentioning that a certain concentration viscosity responded linearly to the applied magnetic field.

The optimization of the damping ratio should be taken into consideration, since a value far greater that the optimum may result in poorer performance [73, 159]. An equivalent damping ratio is adjustable with the yield stress and increases for bigger magnetic fields and is defined in Eq. (35). It also depends on the overall head loss coefficient δ, the standard deviation σ of the fluid velocity $\dot{x}$, the fluid density ρ and previously described parameters and is further explained in Cheng et al. and Wang et al. [155, 159]:

$$\xi_{eq} = \frac{1}{2\sqrt{\pi g L_{eff}}} \left(\delta \sigma_{\dot{x}} + \frac{\tau_{MR} L_M \gamma}{H \rho \sigma_{\dot{x}}} \right) \tag{35}$$

In this case, the first natural frequency of the MF-TLCD applied on the horizontal section is not field-dependent (Eq. (36)).

$$f_{MF-TLCD,H} = \frac{1}{2\pi} \sqrt{\frac{2g}{L}} \tag{36}$$

The experiments carried out by Cheng et al. [159] demonstrate the application of MR fluids on TLCDs is useful specially for larger amplitudes of vibration since higher viscosities prevent heavy sloshing from happening and can mitigate the vibrations for wider bandwidths. Additionally, these devices require less mass compared to traditional TLCDs to achieve similar control efficiency [158].

The advantages regarding the controllable and increased damping from MR-TLCDs are combined with TLCGDs that provide higher frequency applications by Hokmabady et al. [160]. Moreover, the use of MR fluids becomes significant specially for controlling the undesired cavitation phenomenon by a limited velocity.

5.2.4 TLCDs Vertical Section

TLCDs frequency can be controlled if magnetic fields are applied on the column section of the damper [161] as shown in Fig. 23 because upon the application of the magnetic field, the fluid is attracted to the electromagnet and the

position of the free surface can be varied. This introduces a new parameter h_M the magnetic field intensity $H(\eta)$ depends on that describes the distance from the free surface to the center of the magnetic field.

The variations in the natural frequency are studied for different positions and driving current intensities. From the linearized equation of motion of the surface elevation of the fluid (Eq. (37)):

$$\ddot{\eta} \rho AL + \eta A(2\rho g + \mu_0 \chi H(0)\dot{H}(0)) \approx 0 \tag{37}$$

The equation that describes the frequency can be derived in the form (Eq. (38)):

$$f_{MF-TLCD,V} = \frac{1}{2\pi} \sqrt{\frac{2g}{L} + \frac{\mu_0 \chi H(0)\dot{H}(0)}{\rho L}} \tag{38}$$

The magnetic field distribution $H(\eta)$ is described in Eq. (39), where N denotes the number of turns in the coil, I is the electric current intensity, w refers to the width and d_M to the inner diameter of the coil, h_M represents the displacement of the free surface from the coil center and η is the wave surface elevation.

$$H(\eta) = \frac{NI}{2w} \left(\frac{\eta + h_M + w/2}{\sqrt{(\eta + h_M + w/2)^2 + (d_M/2)^2}} - \frac{\eta + h_M - w/2}{\sqrt{(\eta + h_M - w/2)^2 + (d_M/2)^2}} \right) \tag{39}$$

The natural frequency increases with the magnetic field for negative values of h_M. For positive values it decreases unless a strong magnetic field is induced.

6 Final Remarks

TLDs are dissipative devices whose distinguished features make them an attractive damping option. Their working principle is similar to that of a TMD but in this case the
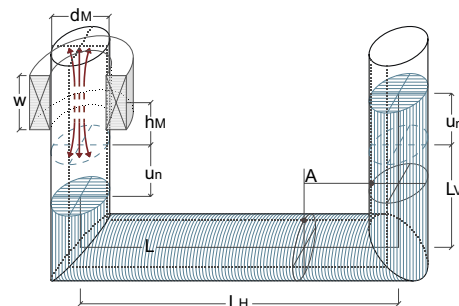

Fig. 23 Schematic of a TLCD with a magnetic field applied on one column

relative movement comes from a fluid that serves as mass, damping and stiffness. Moreover, TLDs can be used not only to mitigate horizontal vibrations but also vertical ones. All these make TLDs worth deeply studying. From early years, different modifications have been implemented in the sought of a better performance.

While some of these improvements are passively developed through geometric or fluid modifications, the inclusion of smart field responsive materials, controlled through magnetic fields, can be beneficial. Since a lack of review is detected in this field, a thorough classification has been proposed depending on the magnetic field configuration that is suitable for different applications depending on the desired effect on its behavior.

On TSDs, a parallel to motion application can be used to enhance or suppress sloshing as required by means of an alternating magnetic field. The same behavior can be obtained for horizontal applications with a certain rotation from the movement axis. It can also be used to modify the amount of sloshing mass, making it possible to adjust the mass ratio and thus providing with the capability to widen and narrow the effective frequency band.

A perpendicular magnetic field applied on TSDs is useful if it is desired to modify the tuning frequency. The magnetic field can restrict the movement of a certain section of the fluid, thus modifying the effective length of the container. This makes it possible to increase the frequency of sloshing or to use a single tank for various frequencies.

If the magnetic field is applied vertically on a TSD, a modified gravity is obtained which can be used to increase the frequency to reach higher values and to control surface motion.

As for TLCDs, if the magnetic field is located on their horizontal section its effect is used to increase the damping, a beneficial effect in which higher viscosities prevent heavy sloshing from happening. When located on the vertical section, the surface elevation can be controlled together with the frequency.

Although TLDs whose working fluid is a smart field responsive fluid has proven to enhance TLDs performance both numerically and experimentally, no real-life implementations have been developed so far to the best of found knowledge. Some of the factors that are determinant are economic issues and the need to ensure power supply for their enhanced functioning. A key future work line consists in selecting and developing appropriate magnetic fluids to be economically competitive while ensuring no sedimentation of the magnetic particles and the use of inorganic materials to prevent biological processes from happening. This can be considered an essential aspect to make magnetic field TLDs competitive with their passive counterparts.

Declarations

Conflict of interest The authors have no competing interests to declare that are relevant to the content of this article. On behalf of all authors, the corresponding author states that there is no conflict of interest.

References

1. Bozzo LM, Barbat AH (2000) Diseño sismorresistente de edificios. Editorial Reverté, S. A, Técnicas convencionales y avanzadas. Barcelona
2. Kareem A, Kijewski T, Tamura Y (1999) Mitigation of motions of tall buildings with specific examples of recent applications. Wind Struct 2(3):201–251
3. Ammann OH, Kármán TV, Glenn K, Woodruff GB (1941) The failure of the Tacoma Narrows Bridge. Tech. Rep. CaltechAUTHORS:20140512-105559175, Federal Works Agency, Washington DC
4. Dallard P, Fitzpatrick T, Flint A, Low A, Smith RR, Willford M, Roche M (2001) London millennium bridge: pedestrian-induced lateral vibration. J Bridge Eng 6(6):412–417
5. Soong T, Spencer B (2002) Supplemental energy dissipation: state-of-the-art and state-of-the-practice. Eng Struct 24(3):243–259
6. Frahm HH (1911) Results of trials of the anti-rolling tanks at sea. J Am Soc Nav Eng 23(2):571–597
7. Bhuta P, Koval L (1966) A viscous ring damper for a freely precessing satellite. Int J Mech Sci 8(5):383–395
8. Alfriend KT (1974) Partially filled viscous ring nutation damper. J Spacecr Rockets 11(7):456–462
9. Vandiver J, Mitome S (1979) Effect of liquid storage tanks on the dynamic response of offshore platforms. Appl Ocean Res 1(2):67–74
10. Modi V, Welt F (1988) Damping of wind induced oscillations through liquid sloshing. J Wind Eng Ind Aerodyn 30(1):85–94

11. Bauer H (1984) Oscillations of immiscible liquids in a rectangular container: a new damper for excited structures. J Sound Vib 93(1):117–133

12. Love J, Tait M (2012) A preliminary design method for tuned liquid dampers conforming to space restrictions. Eng Struct 40:187–197

13. Samali B, Kwok KCS, Tapner D (1992) Vibration control of structures by tuned liquid column dampers. IABSE congress report = Rapport du congrès AIPC = IVBH Kongressbericht 14:461–466

14. Xu YL, Samali B, Kwok KCS (1992) Control of along-wind response of structures by mass and liquid dampers. J Eng Mech 118(1):20–39

15. Alkmim MH, de Morais MVG, Fabro AT (2016) Vibration reduction of wind turbines using tuned liquid column damper using stochastic analysis. J Phys 744:012178

16. Zeng X, Yu Y, Zhang L, Liu Q, Wu H (2015) A new energy-absorbing device for motion suppression in deep-sea floating platforms. Energies 8(1):111–132

17. Hua L, Juang H (2012) Experimental study on the vibration mitigation of offshore tension leg platform system with UWTLCD. Smart Struct Syst 9(1):71–104

18. Nakamura S-I, Fujino Y (2002) Lateral vibration on a pedestrian cable-stayed bridge. Struct Eng Int 12(4):295–300

19. Fujino Y, Pacheco BM, Nakamura S-I, Warnitchai P (1993) Synchronization of human walking observed during lateral vibration of a congested pedestrian bridge. Earthq Eng Struct Dyn 22(9):741–758

20. Tajima J, Ohashi M, Tada K, Yamagishi K (1990) Design and construction of a cable-stayed bridge with mixed structure. IABSE reports = Rapports AIPC = IVBH Reports, vol. 60 of Mixed Structures, including New Materials 60:353–358

21. Tamura Y, Fujii K, Ohtsuki T, Wakahara T, Kohsaka R (1995) Effectiveness of tuned liquid dampers under wind excitation. Eng Struct 17(9):609–621

22. Turkington D (2011) Sky Tower. Wily, Hoboken, pp 304–318

23. Roberts J M (2008) The Brighton i360 Viewing Tower Project, pp. 1–8

24. Hasan A (2008) Inspiring Innovation - One King West Tower. Structure Magazine, pp 34–37

25. Simpson R, Simpson G (2001) Buildings: One Wall Center, Vancouver.https://www.canadianconsultingengineer.com/features/buildings-one-wall-centre-vancouver/. Accessed: 2023-03-20

26. Klemencic R, Hooper J, Johansson O(2008) One Rincon Hill: Raising the Bar, pp. 1–11. 2008

27. D'Huy (2006) Engineering, Comcast Center - Tuned Liquid Column Damper.https://www.dhuy.com/comcast-center-tuned-liquid-column-damper. Accessed: 2023-03-20

28. Feldmann M, Baitinger M, Vaudeville B (2002) Le grand écran de verre de la nouvelle église "notre dame de pentecôte" à paris-la défense. Construction Métallique 2:40–55

29. PMI Engineers, "My World and Your World Eva Rothschild sculpture." https://pmiengineers.com/Eva-Rothschild-Sculpture, 2020. Accessed: 2023-01-12

30. Frahm H (1909) "Device for damping vibrations of bodies," . US Patent US989958A

31. Christopoulos C, Filiatrault A (2006) Principles of passive supplemental damping and seismic isolation

32. Weber B, Feltrin G (2010) Assessment of long-term behavior of tuned mass dampers by system identification. Eng Struct 32(11):3670–3682

33. Tubino F, Piccardo G (2015) Tuned mass damper optimization for the mitigation of human-induced vibrations of pedestrian bridges. Meccanica 50(3):809–824

34. Garcia-Troncoso N, Ruiz-Teran A, Stafford P J(2020) Attenuation of pedestrian-induced vibrations in girder footbridges using tuned-mass dampers. Adv Bridge Eng 1(1):1-14

35. Warburton GB (1982) Optimum absorber parameters for various combinations of response and excitation parameters. Earthq Eng Struct Dyn 10(3):381–401

36. Sadek F, Mohraz B, Taylor AW, Chung RM (1997) A method of estimating the parameters of tuned mass dampers for seismic applications. Earthq Eng Struct Dyn 26(6):617–635

37. Wang D, Tse TK, Zhou Y, Li Q (2014) Structural performance and cost analysis of wind-induced vibration control schemes for a real super-tall building. Struct Infrastruct Eng 11(8):990–1011

38. Yu J-K, Wakahara T, Reed DA (1999) A non-linear numerical model of the tuned liquid damper. Earthq Eng Struct Dyn 28(6):671–686

39. Housner GW (1957) Dynamic pressures on accelerated fluid containers. Bull. Seismol. Soc. Am. 47(1):15–35

40. Housner GW (1963) The dynamic behavior of water tanks. Bull. Seismol. Soc. Am. 53(2):381–387

41. Accioly M. E, Melo L P C, de Araújo T D (2017) Analytical evaluation of water supply tanks as dampers. Proceedings of the XXXVIII Iberian Latin American Congress on Computational Methods in Engineering, ABMEC Brazilian Association of Computational Methods in Engineering

42. Sun L, Fujino Y, Pacheco BM, Isobe M (1989) Nonlinear waves and dynamic pressures in rectangular tuned liquid damper (TLD). simulation and experimental verification. Doboku Gakkai Ronbunshu 410(12):81–92

43. Fujino Y, Sun L, Pacheco BM, Chaiseri P (1992) Tuned liquid damper (TLD) for suppressing horizontal motion of structures. J Eng Mech 118(10):2017–2030

44. Sun LM, Fujino Y, Chaiseri P, Pacheco BM (1995) The properties of tuned liquid dampers using a TMD analogy. Earthq Eng Struct Dyn 24(7):967–976

45. Fujino Y, Pacheco BM, Chaiseri P, Sun L (1988) Parametric studies on tuned liquid damper (TLD) using circular containers by free-oscillation experiments. Doboku Gakkai Ronbunshu 1988(398):177–187

46. Reed D, Yu J, Yeh H, Gardarsson S (1998) Investigation of tuned liquid dampers under large amplitude excitation. J Eng Mech 124(4):405–413

47. Morsy H (2010) A Numerical Study of the Performance of Tuned Liquid Dampers. Master's thesis, McMaster University, Hamilton

48. Li SJ, Li GQ, Tang J, Li QS (2002) Shallow cylindrical tuned liquid damper for vibration control of high-rise structures. Struct Des Tall Build 11(4):295–308

49. Kim Y-M, You K-P, Cho J-E, Hong D-P (2006) The vibration performance experiment of tuned liquid damper and tuned liquid column damper. J Mech Sci Technol 20(6):795–805

50. Calvi G M, Nascimbene R(2011) Progettazione sismica dei serbatoi. Pavia: IUSS Press pp. 537–672

51. Priestley MJN, Wood JH, Davidson BJ (1986) Seismic design of storage tanks. Bull. N. Z. Soc. Earthq. Eng. 19:272–284

52. ACI Committee 350 (2006) Seismic design of liquid-containing concrete structures (ACI 350.3-06): an ACI Standard. American Concrete Institute

53. Miles J.W. (1967) Surface-wave damping in closed basins, Proceedings of the Royal Society of London. Series A Math Phys Sci 297(1451):459–475

54. Sun L (1991) Semi-analytical modelling of tuned liquid damper (TLD) with emphasis on damping of liquid sloshing. PhD thesis, University of Tokyo

55. Habenberger J (2015) Fluid damping of cylindrical liquid storage tanks. SpringerPlus, Cham 515(4)

56. Sun L, Fujino Y, Pacheco B, Chaiseri P (1992) Modelling of tuned liquid damper (TLD). J Wind Eng Ind Aerodyn 43(1):1883–1894

57. Tait MJ (2008) Modelling and preliminary design of a structure-TLD system. Eng Struct 30(10):2644–2655

58. Sun L, Kikuchi T, Goto Y, Hayashi M (1998) Tuned liquid damper (tld) using heavy mud. Trans Built Environ 35:87–96

59. Tait M J, Damatty A A E, Isyumov N (2002) The Dynamic Properties of a Tuned Liquid Damper Using an Amplitude Dependent Tuned Mass Damper, in 4th Structural Speciality Conference of the Canadian Society for Civil Engineering

60. EN 1998-4:2006 (2021) Eurocode 8: Design of structures for earthquake resistance. Part 4: Silos, tanks and pipelines. UNE Normalización Española

61. Hartog JPD (1947) Mechanical VIbrations 3rd edn. McGraw-Hill Book Company, New York

62. Ohno K-I, Sawada T (2010) An effect of vertical sloshing on a fluid pressure and a surface displacement in a tuned magnetic fluid damper. International Journal of Applied Electromagnetics and Mechanics 33(3–4):1411–1416

63. Konar T, Ghosh A D (2022) A review on various configurations of the passive tuned liquid damper. J Vib Control 0(0):10775463221074077

64. Farshidianfar A, Oliazadeh P, Farivar H R (2009) Optimal parameter's design in Tuned Liquid Column Damper, in 17th. Annual (International) Conference on Mechanical Engineering-ISME2009, (Tehran)

65. Behbahan HP, Bin-Adnan A, Shad H (2012) Effectiveness of tuned liquid column dampers on vibration behavior of one-story steel structure under harmonic force and an earthquake record. Aust J Basic Appl Sci 6(13):41–47

66. Wu JC, Shih MH, Lin YY, Shen YC (2005) Design guidelines for tuned liquid column damper for structures responding to wind. Eng Struct 27(13):1893–1905

67. Gao H, Kwok K, Samali B (1997) Optimization of tuned liquid column dampers. Eng Struct 19(6):476–486

68. Balendra T, Wang C, Cheong H (1995) Effectiveness of tuned liquid column dampers for vibration control of towers. Eng Struct 17(9):668–675

69. Yalla SK, Kareem A (2000) Optimum absorber parameters for tuned liquid column dampers. J Struct Eng 126(8):906–915

70. Won AY, Pires JA, Haroun MA (1997) Performance assessment of tuned liquid column dampers under random seismic loading. Int J Non-Linear Mech 32(4):745–758

71. (1992) "DOE Fundamentals Handbook: Thermodynamics, Heat Transfer, and Fluid Flow, volume 3," Tech. Rep. DOE-HDBK-1012/3-92, U.S. Department of Energy, Washington DC,

72. Hitchcock P, Kwok K, Watkins R, Samali B (1997) Characteristics of liquid column vibration absorbers (LCVA)-I. Eng Struct 19(2):126–134

73. Sun L, Fujino PBMY, Chaiseri P (1989) Effects of liquid viscosity on TLD performance-Experiment and simulation. In: Proceedings of Japan Society of Civil Engineers, pp 732–733

74. Das S, Choudhury S (2017) Seismic response control by tuned liquid dampers for low-rise RC frame buildings. Aust J Struct Eng 18(2):135–145

75. Ocak A, Bekdaş G, Nigdeli SM, Kim S, Geem ZW (2022) Optimization of tuned liquid damper including different liquids for lateral displacement control of single and multi-story structures. Buildings 12(3):377

76. Modi V, Akinturk A (2002) An efficient liquid sloshing damper for control of wind-induced instabilities. J Wind Eng Ind Aerodyn 90(12):1907–1918

77. Agresta A, Cavalagli N, Biscarini C, Ubertini F (2021) Effect of bottom geometry on the natural sloshing motion of water inside tanks: An experimental analysis. Appl Sci 11(2):605

78. Cavalagli N, Agresta A, Biscarini C, Ubertini F, Ubertini S (2021) Enhanced energy dissipation through 3D printed bottom geometry in Tuned Sloshing Dampers. J Fluids Struct 106:103377

79. McNamara KP, Love JS, Tait MJ (2022) Numerical investigation of the response of structures equipped with a limited freeboard tuned liquid damper. J Fluids Struct 108:103426

80. Tait MJ, Isyumov N, Damatty AA (2006), Tuned Liquid Dampers to Mitigate Wind-Induced Motions of Buildings, pp 1–10

81. Ruiz R, Lopez-Garcia D, Taflanidis A (2014) An innovative type of Tuned Liquid Damper, in NCEE 2014 - 10th U.S. National Conference on Earthquake Engineering: Frontiers of Earthquake Engineering

82. Ruiz RO, Taflanidis AA, Lopez-Garcia D (2016) Characterization and design of tuned liquid dampers with floating roof considering arbitrary tank cross-sections. J Sound Vib 368:36–54

83. Fediw A, Isyumov N, Vickery B (1995) Performance of a tuned sloshing water damper. J Wind Eng Ind Aerodyn 57(2):237–247

84. Lee D, Ng M (2010) Application of tuned liquid dampers for the efficient structural design of slender tall buildings. Counc Tall Build Urban Habitat J (IV): 30–36

85. Robinson JK, Gamble SL, Myslimaj BM (2007) Supplemental damping and using tuned sloshing dampers. Struct Mag 6:14–18

86. Frandsen J (2012) Sloshing in tanks: assessment of traditional and lattice Boltzmann solutions. In: International Conference on Violent Flows

87. Vafaei M, Pabarja A, Alih SC (2021) An innovative tuned liquid damper for vibration mitigation of structures. Int J Civil Eng 19(9):1071–1090

88. Colwell S, Basu B (2008) Experimental and theoretical investigations of equivalent viscous damping of structures with TLCD for different fluids. J Struct Eng 134:154–163

89. Reiterer M, Kluibenschedl A (2010) "Liquid damper for reducing vertical and/or horizontal vibrations in a building or machine structure," . US Patent US 2010/0200348 A1

90. Tanveer M, Usman M, Khan IU, Farooq SH, Hanif A (2020) Material optimization of tuned liquid column ball damper (TLCBD) for the vibration control of multi-storey structure using various liquid and ball densities. J Build Eng 32:101742

91. Hitchcock P, Kwok K, Watkins R, Samali B (1997) Characteristics of liquid column vibration absorbers (LCVA)-II. Eng Struct 19(2):135–144

92. Chaiviriyawong P, Webster WC, Pinkaew T, Lukkunaprasit P (2007) Simulation of characteristics of tuned liquid column damper using a potential-flow method. Eng Struct 29(1):132–144

93. Smith MJ, Kobine JJ, Davidson FA (2005) Controlling beat phenomena in coupled systems using asymmetric tuned liquid column dampers. WIT Trans Built Environ 84:8

94. Park BJ, Lee YJ, Park MJ, Ju YK (2018) Vibration control of a structure by a tuned liquid column damper with embossments. Eng Struct 168:290–299

95. Rozas L, Boroschek RL, Tamburrino A, Rojas M (2016) A bidirectional tuned liquid column damper for reducing the seismic response of buildings. Struct Control Health Monit 23(4):621–640

96. Min K-W, Kim J, Kim Y-W (2014) Design and test of tuned liquid mass dampers for attenuation of the wind responses of a full scale building. Smart Mater Struct 23:4

97. Zhou Y, Qian L, Bai W (2023) Sloshing dynamics of a tuned liquid multi-column damper for semi-submersible floating offshore wind turbines. Ocean Eng 269:113484

98. Ding H, Wang JT, Lu LQ, Zhu F (2020) A toroidal tuned liquid column damper for multidirectional ground motion-induced vibration control. Struct Control Health Monit 27:8

99. Ding H, Wang JT, Wang JW, Jia RF (2021) Optimized parameters of toroidal tuned liquid column dampers for multidirectional pitching vibration mitigation of structures. Struct Multidiscip Optim 64(6):3401–3421

100. Jaksic V, Wright CS, Murphy J, Afeef C, Ali SF, Mandic DP, Pakrashi V (2015) Dynamic response mitigation of floating wind turbine platforms using tuned liquid column dampers. Philos Trans Royal Soc A 373(2035):20140079

101. Ahadi P, Mohebbi M, Shakeri K (2012) Using optimal multiple tuned liquid column dampers for mitigating the seismic response of structures. ISRN Civil Eng 2012:592181

102. Gao H, Kwok K, Samali B (1999) Characteristics of multiple tuned liquid column dampers in suppressing structural vibration. Eng Struct 21(4):316–331

103. Cao L, Gong Y, Ubertini F, Wu H, Chen A, Laflamme S (2020) Development and validation of a nonlinear dynamic model for tuned liquid multiple columns dampers. J Sound Vib 487:115624

104. Wang Z, Cao L, Ubertini F, Laflamme S (2021) Numerical investigation and design of reinforced concrete shear wall equipped with tuned liquid multiple columns dampers. Shock Vib 2021:6610811

105. Wang Z, Micheli L, Ubertini F, Laflamme S (2022) Risk-informed design optimization of vertically distributed tuned liquid wall dampers for multihazard mitigation. J Struct Eng 148(3):04021295

106. Al-Saif KA, Aldakkan KA, Foda MA (2011) Modified liquid column damper for vibration control of structures. Int J Mech Sci 53(7):505–512

107. Tanveer M, Usman M, Khan IU, Ahmad S, Hanif A, Farooq SH (2019) Application of tuned liquid column ball damper (TLCBD) for improved vibration control performance of multi-storey structure. PLoS One 14(10):e0224436

108. Shah MU, Usman M, Farooq SH, Kim IH (2022) Effect of tuned spring on vibration control performance of modified liquid column ball damper. Appl Sci 12(1):103390

109. Shah MU, Usman M, Farooq SH, Rizwan M (2023) Spring-controlled modified tuned liquid column ball damper for vibration mitigation of structures. J Sound Vib 545:117443

110. Reiterer M (2004) Control of pedestrian-induced bridge vibrations by tuned liquid column dampers. In: Proceedings of the Third European Conference on Structural Control

111. Reiterer M, Wendner R, Hoffman S, Strauss A, Bergmeister K (2007) Tuned liquid column dampers-effective damping of vertical vibrations. In: 3rd International Conference on Structural Health Monitoring of Intelligent Infrastructure

112. Hochrainer MJ (2005) Tuned liquid column damper for structural control. Acta Mechanica 175(3):57–76

113. Sowayan AS (2020) Stiffness of a nonlinear adiabatic polytropic air spring model: quantitative and conductive investigation. Int Rev Model Simul 13(3):177–184

114. Ye J, Huang H, He C, Liu G (2018) Analysis of vertical stiffness of air spring based on finite element method. In: MATEC Web of Conferences, The 4th International Conference on Mechatronics and Mechanical Engineering (ICMME 2017), vol 153, p 06006, EDP Sciences

115. Hochrainer MJ, Fotiu PA (2018) Design of coupled tuned liquid column gas dampers for multi-mode reduction in vibrating structures. Acta Mechanica 229:911–928

116. Hokmabady H, Mojtahedi A, Mohammadyzadeh S (2022) Development of a novel tuned liquid multiple columns gas damper under wave and earthquake incidence. Appl Ocean Res 118:102956

117. Phulé PP (2001) Magnetorheological (mr) fluids: principles and applications. Smart Mater Bull 2001(2):7–10

118. Phulé PP, Ginder JM (1998) The materials science of field-responsive fluids. MRS Bull 23(8):19–22

119. Genc S, Derin B (2012) Field responsive fluids - a review. Key Eng Mater 521:87–99

120. Hajalilou A, Mazlan SA, Lavvafi H, Shameli K (2016) Insight into the Field Responsive Fluids. Springer Science and Business Media B.V., Berlin, pp 127–134

121. Olabi AG, Grunwald A (2007) Design and application of magneto-rheological fluid. MaterDesign 28(10):2658–2664

122. Ahn KK, Truong DQ, Islam MA (2009) Modeling of a magneto-rheological (MR) fluid damper using a self tuning fuzzy mechanism. J Mech Sci Technol 23(5):1485–1499

123. Sassi S, Cherif K, Thomas M (2003) On the design and testing of a smart car damper based on electro-rheological technology. Smart Mater Struct 12(6):873–880

124. Xu YL, Qu WL, Ko JM (2000) Seismic response control of frame structures using magnetorheological/electrorheological dampers. Earthq Eng Struct Dyn 29(5):557–575

125. Dyke SJ, Spencer BF Jr, Sain MK, Carlson JD (1998) An experimental study of MR dampers for seismic protection. Smart Mater Struct 7(5):693–703

126. Lenggana BW, Ubaidillah U, Imaduddin F, Choi SB, Purwana YM, Harjana H (2021) Review of magnetorheological damping systems on a seismic building. Appl Sci 11(19):9339

127. Morita K, McCabe S (2004) US-Japan cooperative structural testing research program on smart structural systems. In: UJNR Panel on Wind and Seismic Effects. Panel Update, vol 1, no 5

128. Spencer BF, Nagarajaiah S (2003) State of the art of structural control. J Struct Eng 129(7):845–856

129. Cesmeci S, Gordaninejad F, Ryan KL, Eltahawy W (2019) Design of a fail-safe magnetorheological-based system for three-dimensional earthquake isolation of structures. Mechatronics 64:102296

130. Sharma S, Khurana S (2017) Investigation on Magnetorheological Damper for Its Various Applications. Int J Eng Technol Manag Appl Sci 6:10–15

131. Çengel Y A, Cimbala J M(2006) Fluid Mechanics. Fundamentals and applications. McGraw-Hill series in Mechanical Engineering

132. Lopez-Lopez MT, Duran JD, Zubarev AY (2022) Rheological Analysis of Magnetorheological Fluids. Elsevier, Amsterdam, pp 237–247

133. Hajalilou A, Mazlan SA, Lavvafi H, Shameli K (2016) Magnetorheological (MR) Fluids. Springer Science and Business Media B.V, Berlin, pp 13–50

134. Bossis G, Lacis S, Meunier A, Volkova O (2002) Magnetorheological fluids. J Magn Magn Mater 252:224–228

135. Hajalilou A, Mazlan SA, Lavvafi H, Shameli K (2016) Electorheological (ER) Fluids. Springer Science and Business Media B.V., Berlin, pp 95–107

136. Rosensweig RE (1985) Ferrohydrodynamics. Dover Publications Inc., New York

137. Hajalilou A, Mazlan SA, Lavvafi H, Shameli K (2016) Ferrofluids. Springer Science and Business Media B.V., Berlin, pp 115–119

138. Doganay S, Alsangur R, Turgut A (2019) Effect of external magnetic field on thermal conductivity and viscosity of magnetic nanofluids: A review. Mater Res Express 6(11):112003

139. Genc S, Derin B (2014) "Synthesis and rheology of ferrofluids: a review," Current Opinion in Chemical Engineering. Biol Eng Mater Eng 3:118–124

140. Mesquida CD, Lässig JL (2012) Introducción a los fluidos magnetoreológicos con aplicaciones en ingeniería. Revista Iberoamericana de Ingeniería Mecánica 16(1):27–36

141. Cho MY, Kim JS, Choi SB, Kim GW (2016) Non-contact tunable damping of a cantilever beam structure embedded with photo-rheological fluids. Smart Mater Struct 25(2):025022

142. Sudo S, Hashimoto H, Ikeda A, Katagiri K (1987) Some studies of magnetic liquid sloshing. J Magn Magn Mater 65(2):219–222

143. Zelazo RE, Melcher JR (1969) Dynamics and stability of fer-rofluids: surface interactions. J Fluid Mech 39(1):1–24

144. Sawada T, Kikura H, Shibata S, Tanahashi T (1993) Lateral sloshing of a magnetic fluid in a container. J Magn Magn Mater 122(1):424–427

145. Sawada T, Tanahashi T, Kikura H (1999) Kinematic characteristics of magnetic fluid sloshing in a rectangular container subject to non-uniform magnetic fields. Exp Fluids 26(3):215–221

146. Abé M, Fujino Y, Sano Y (1997) Vibration control by active tuned liquid damper using magnetic fluid. In: Proceedings of DETC'97, ASME Design Engineering Technical Conferences, vol. Volume 1B: 16th Biennial Conference on Mechanical Vibration and Noise of International Design Engineering Technical Conferences and Computers and Information in Engineering Conference

147. Horie S, Shimoda M, Ohno K-I, Nakamura J, Sawada T (2007) Effective method of applying magnetic field on a tuned liquid damper using a magnetic fluid. Int J Appl Electromagn Mech 25:139–143

148. Abe M, Fujino Y, Kimura S (1998) Active tuned liquid damper (TLD) with magnetic fluid,'' in Smart Structures and Materials 1998: Smart Structures and Integrated Systems (M. E. Regel-brugge, ed.). Society of Photo-Optical Instrumentation Engineers (SPIE) Conference Series 3329:620–623

149. Ohira Y, Houda H, Sawada T (2001) Effect of magnetic field on a tuned liquid damper using a magnetic fluid. Int J Appl Electro-magn Mech 13:71–78

150. Sakamoto D, Oshima N, Fukuda T (2001) Tuned sloshing damper using electro-rheological fluid. Smart Mater Struct 10(5):960–963

151. Ohno K, Shimoda M, Sawada T (2008) Optimal design of a tuned liquid damper using a magnetic fluid with one electromagnet. J Phys 20(20):204146

152. Ohno KI, Suzuki H, Sawada T (2011) Analysis of liquid sloshing of a tuned magnetic fluid damper for single and co-axial cylindrical containers. J Magn Magn Mater 323(10):1389–1393

153. Zahrai S M, Abbasi S (2010) Study on possibility of using tuned liquid dampers (TLD) in high frequency structures. In: 17th International Congress on Sound and Vibration (ICSV17)

154. Frandsen, JB (2008) Sloshing in tanks in a magnetic field. In: Zolotarev, Horacek (eds) Flow induced vibration. Institute of Thermomechanics

155. Wang JY, Ni YQ, Ko JM, Jr BFS (2005) Magneto-rheological tuned liquid column dampers (MR-TLCDs) for vibration miti-gation of tall buildings: Modelling and analysis of open-loop control. Comput Struct 83(25–26):2023–2034

156. Hajalilou A, Mazlan SA, Lavvafi H, Shameli K (2016) Models and Modes in MR Fluids. Springer Science and Business Media B.V., Berlin, pp 51–65

157. Jolly MR, Bender JW, Carlson JD (1999) Properties and appli-cations of commercial magnetorheological fluids. J Intell Mater Syst 10(1):5–13

158. Roychowdhury D, Gur S (2022) MR tuned liquid colum damper (MR-TLCD) for seismic vibration control,'' in ASPS Confer-ence Proceedings. Proceedings of the 12th Structural Engineer-ing Convention 1(12):1139–1147

159. Cheng CW, Lee HH, Luo YT (2015) Experimental study of con-trollable MR-TLCD applied to the mitigation of structure vibra-tion. Smart Struct Syst 15(6):1481–1501

160. Hokmabady H, Mohammadyzadeh S, Mojtahedi A (2019) Sup-pressing structural vibration of a jacket-type platform employing a novel Magneto-Rheological Tuned Liquid Column Gas Damper (MR-TLCGD). Ocean Eng 180:60–70

161. Masuda H, Oyamada T, Sawada T (2013) Experimental study on damping characteristics of the tuned liquid column damper with magnetic fluid. J Phys 412(1):012049